NANO LETTERS

2003
Vol. 3, No. 4
543−547

Structural Tunability of the Plasmon Resonances in Metallic Nanoshells

E. Prodan and P. Nordlander*

Department of Physics and Rice Quantum Institute, Rice University, Houston, Texas 77251

Received January 15, 2003; Revised Manuscript Received February 10, 2003

ABSTRACT

Using the time-dependent LDA method, we investigate the tunability of the optical polarizability of small metallic nanoshells. We show that the energies of the two dipolar plasmon resonances vary with the ratio of shell thickness to particle radius in a manner similar to what has been predicted using classical Mie scattering and semiclassical models for uniform metallic shell structures.

In the past few years, a considerable amount of research has been devoted to the optical properties of nanoparticles.[1,2] Semiconductor nanocrystals, or quantum dots, have received extensive attention due to the dramatic effects of confinement on electron−hole pair excitations within the particle due primarily to particle size. By contrast, the optical response of metallic nanoparticles has been thought to span a continuum from a regime where quantum effects dominate (for nanoparticles nominally <100 atoms) to a classical regime where the optical response is determined by the properties of the nanoparticle plasmon. The plasmon response in this regime has typically been assumed to be classical and has been interpreted using Mie scattering theory.

A particularly interesting and possibly very useful new type of nanoparticle is the metallic nanoshell.[3] The particles consist of a thin gold or silver shell around a dielectric core.[4−7] Mie scattering theory predicts that by varying the ratio of the shell thickness with respect to the overall diameter of the particle the plasmon frequencies of the nanoshells can be placed at arbitrary wavelengths between the mid-infrared and the UV region of the optical spectrum.[8−10] The structural tunability of the plasmon frequencies of these unique nanoparticles has been experimentally verified in a series of studies where monodisperse nanoshells of different shell thicknesses and core sizes have been fabricated and characterized with optical measurements.[11] This tunable plasmon resonance is not only of fundamental interest for nanocavity physics[12] but also makes these nanoparticles particularly attractive for applications such as resonant photooxidation inhibitors[13] and optical triggers for opto-mechanical materials,[14] drug delivery implants,[15] environmental sensors,[16] and Raman sensors.[17]

The electronic and optical properties of metallic shell structures have also been of interest in the historical context of atomic physics. A general semiclassical approach (SCA) was developed and applied to describe collective resonances in inner atomic shells of heavy atoms.[18,19] This model and extensions of it have subsequently been applied to the calculation of the optical absorption spectra of other electronic shell structures such as the C_{60} molecule.[20−22] For a spherical shell geometry with a step-function charge density (uniform electron density in the shell and no electron spillout), SCA predicts two collective oscillation modes for each component of angular momentum.[18] The energies of these plasmons are

$$\omega_{l\pm}^{2} = \omega_s^2 \left[1 \pm \frac{1}{2l+1}\sqrt{1 + 4l(l+1)x^{2l+1}}\right] \qquad (1)$$

where $\omega_s = \sqrt{2\pi e^2 n_0/m}$ is the surface plasmon energy and x is the aspect ratio defined as the ratio between the inner and outer radii of the metallic shell. The ω_{l-} mode corresponds to a symmetric coupling between surface plasmons on the inner and outer surfaces of the shell and the higher-energy ω_{l+} mode corresponds to an antisymmetric coupling. Equation 1 can also be derived using classical Mie scattering with a Drude dielectric function in the limit when the nanoshell is much smaller than the wavelength of the light.

Approaches such as SCA, classical Mie scattering theory, or the finite difference time domain have been proven to describe the optical response of the metallic nanoshells accurately. These formalisms require a critical input, which is the dielectric function of the metallic phase. The dielectric function assumed in these classical calculations is that of the bulk metal. Corrections that account for surface scatterings (finite size) have also been considered and have been shown to improve the classical results. With all of the success of the classical theories, a first principles description is desirable for several reasons. First, it will provide the dielectric function, which, as we already mentioned, can be

* Corresponding author. E-mail: nordland@rice.edu.

10.1021/nl034030m CCC: $25.00
Published on Web 02/25/2003

used in classical simulations. Second, a full quantum description can incorporate effects that cannot be treated classically such as molecules chemically binding to the surface or the presence of bias magnetic or electric fields.

To date, there have been only a few quantum mechanical calculations of the optical response of nanoshells. In particular, there has been no first principles investigation of the dependence of the plasmon resonances on the nanoshell aspect ratio. In this paper, we apply the time-dependent local density approximation (TDLDA) to investigate the structural tunability of metallic nanoshells. We show that indeed the plasmon energies depend on the aspect ratio of the nanoshell in a manner similar to what has been predicted by classical Mie theory and the SCA, thus proving the reliability of the model. An efficient numerical implementation of the TDLDA method for these relatively large systems has been described previously.[23−27] The metallic nanoshell is treated within the jellium model. The electronic structure is determined by solving the Kohn−Sham equations

$$\left(-\frac{1}{2}\vec{\nabla^2} + V + \upsilon_{\mathrm{C}} + \upsilon_{\mathrm{xc}}(n)\right)\eta_i = \epsilon_i \eta_i \qquad (2)$$

where υ_{C} is the Coulomb potential generated by the charge density n and by the positive background charge and υ_{xc} is the exchange correlation potential.[28] The metallic shell is modeled using $r_{\mathrm{s}} = 3$ (au), which is appropriate for bulk gold. This r_{s} corresponds to a surface plasmon energy of $\omega_{\mathrm{s}} = 6.4$ eV and a bulk plasmon energy of $\omega_{\mathrm{p}} = 9$ eV. The background potential V represents the interaction of electrons with the atoms and is adjusted such that the highest occupied electronic level of the nanoshell matches the work function of gold (5.4 eV). This choice of parameters has been shown to provide a reasonable description of the plasmon resonances in small metallic nanoshells.[26] Equation 2 is solved self-consistently using conventional methods. The frequency-dependent polarizability is calculated from

$$\alpha(\omega) = \frac{4\pi}{3}\int \mathrm{d}r\, r^3\, \alpha(r, \omega) \qquad (3)$$

where $\alpha(r, \omega)$ is the local polarizability.[24] The TDLDA self-consistent equation for the local polarizability $\alpha(r, \omega)$ is

$$\alpha(r, \omega) = \alpha^0(r, \omega) + \frac{4\pi}{3}\int \mathrm{d}r_1 r_1^2 \int \mathrm{d}r_2\, r_2^2 \prod_{l=1}^{0}(r, r_1; \omega)\frac{r_<}{r_>^2}\alpha(r_2, \omega) + \int \mathrm{d}r_1\, r_1^2 \prod_{l=1}^{0}(r, r_1; \omega)\upsilon'_{\mathrm{xc}}(n(r_1))\,\alpha(r_1, \omega) \qquad (4)$$

where $r_>$ and $r_<$ represents the maximum and minimum of r_1 and r_2, respectively, and $\alpha^0(r, \omega)$ is the polarizability of the independent electrons.[29] The quantity $\Pi_{l=1}^0$ is the $l = 1$ component of the response function for the independent electrons.[30] The photoabsorption cross section of the nanoshell σ_{abs} is related to its polarizability $\alpha(\omega)$ through

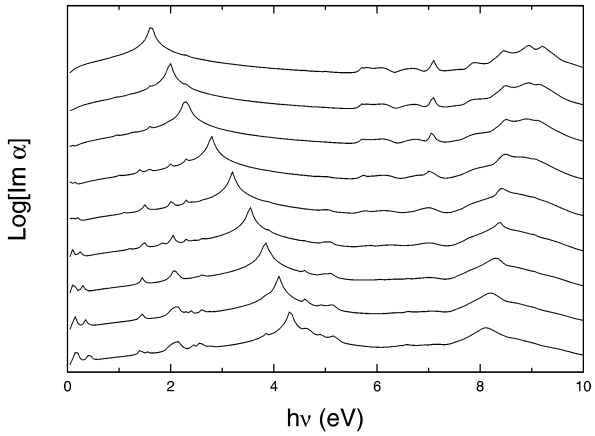

Figure 1. Calculated optical absorption log[Im[$\alpha(h\nu)$]] as a function of photon energy $h\nu$ for several nanoshells of thickness 17 au and varying sizes. The optical absorption spectra for each nanoshell has been offset for clarity. In order from the bottom curve and upward, the nanoshells are of sizes (25.5, 42.5), (31.6, 58.6), (39.7, 58.7), (51.0, 68.0), (68.0, 85.0), (96.3, 113.3), (153.0, 170.0), (209.7, 226.7) and (323.0, 340.0) au, respectively.

$$\sigma_{\mathrm{abs}}(\omega) = \frac{2\pi}{c}\omega Im[\alpha(\omega)]$$

In this paper, we study several nanoshells of varying aspect ratios. We refer to the different nanoshells using the notation (a, b), where a and b are the inner and outer radii of the shell, respectively. The size of the nanoshells will be kept much smaller than the wavelength of the photons so that retardation effects can be neglected.[2] In Figure 1, we show the calculated frequency dependence of Im[$\alpha(\omega)$] for nine nanoshells with a thickness of 17 au but with a varying overall size. The calculated spectra are shown on a logarithmic scale to enhance the details. The dominant features in each spectra are two prominent peaks corresponding to the symmetric-shell plasmon mode ω_{1-} and the antisymmetric ω_{1+} mode. Single-particle excitations show up as narrow spikes in the low-energy region (below the ionization potential of 5.4 eV) and are strongest for the smallest nanoshells. The curves also display several collective features around the bulk plasmon mode at an energy of $\omega_{\mathrm{p}} = 9$ eV, which will be further discussed below. For the largest nanoshells, which contain around 2×10^5 electrons, the single electron levels start to approach a continuum. Consequently, the curves are relatively smooth, and the optical response is dominated by collective excitations. The Figure clearly shows that the energies of the dipolar plasmon resonances depend on the aspect ratio of the nanoshell.

In Figure 2, we show a comparison of the energies of the two dipolar plasmon resonances calculated using TDLDA and the SCA (eq 1) as a function of the aspect ratio $x = a/b$ of the nanoshell. For the three largest nanoshells, the ω_+ resonance lies very close to the aforementioned collective modes near the bulk plasmon frequency, and it is difficult to assign a precise value. Our procedure for determining the ω_+ value here is to fit a Lorentzian to the multiple peak structure and let its center be identified as the energy of the ω_+ mode. It can be seen that the calculated plasmon energies follow the predictions of the SCA result for a uniform

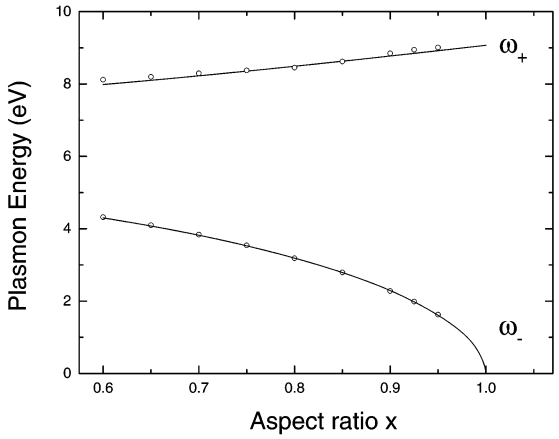

Figure 2. Comparison of calculated symmetric ω_- and antisymmetric ω_+ plasmon resonances (○) for the nanoshells in Figure 1 as a function of their aspect ratio $x = {}^{a}/_{b}$ with the result from the semiclassical approximation (eq 1) (—).

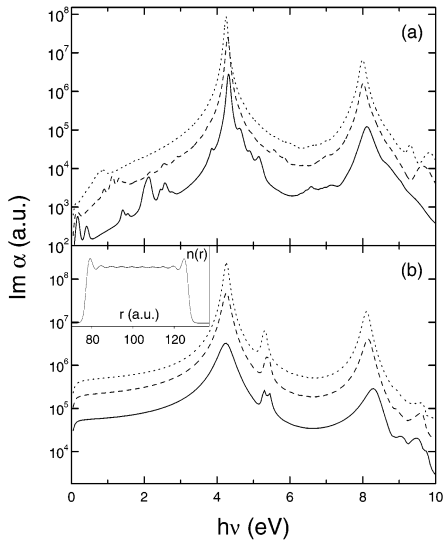

Figure 3. (a) Calculated optical absorption $Im[\alpha(h\nu)]$ as a function of photon energy $h\nu$ for three nanoshells with the same aspect ratio $x = 0.6$ but different sizes (25.5, 42.5) au (—), (51, 85) au (– – –), and (76.5, 127.5) au (···). (b) Results obtained using the semiclassical theory (eqs 5 and 6) and the calculated electron-density distributions. The inset shows the calculated $n(r)$ for the (76.5, 127.5) au nanoshell.

electron distribution in the shell (eq 1) when the aspect ratio of the nanoshell is varied. The agreement between the two calculations is remarkable given the crude approximations underlying the SCA, specifically, the neglect of quantum mechanical effects such as quantum size effects, discrete electronic structure, and screening.

The physical feature that makes the nanoshells attractive for practical applications is that there is only one parameter that controls the position of the absorption peaks. Classical models show that the energy of the plasmon modes depends only on the aspect ratio of the shell and is independent of the overall size of the particle. In the following, we apply TDLDA to a series of nanoshells with the same aspect ratio but different overall sizes. In Figure 3a, we show the calculated optical absorption spectra $Im[\alpha(\omega)]$ for three different nanoshells. As in Figure 1, it can be seen that for the smallest nanoshell relatively strong single-particle excitations are present in the spectral region up to the ionization potential at 5.4 eV. For the larger nanoshells, the spectral weight of such excitations are decreased because of the increased strength of the collective modes ω_- and ω_+. The calculated plasmon energies show only a weak size dependence with a slight red shift of the plasmon energies with increasing size of the shell. Such a size-dependent shift is absent for the simple expression of the plasmon energies (eq 1) of a uniform nanoshell but could be caused by a size-dependent change in the electron-density distribution.[21] To investigate this effect, we apply the SCA to the electron-density profiles calculated for each nanoshell using our LDA method. The SCA is obtained from RPA in the limit where the energy of quantum excitations is much smaller than the external excitation frequency. In this limit, the response function depends only on the density of electrons, and the equation for the local polarizabilty, written in atomic units, becomes[18]

$$\alpha(r, \omega) = -\frac{4\pi}{3(\omega^2 - \omega_{pl}^2(r))}\frac{dn}{dr} \left[1 - \int_0^\infty dr'\, G(r, r')\, \alpha(r', \omega)\right] \quad (5)$$

where

$$G(r, r') = 2\theta(r - r')\left(\frac{r'}{r}\right)^3 - \theta(r' - r) \quad (6)$$

The local plasmon energy $\omega_{pl}(r)$ is linked to the local density of electrons $n(r)$ through $\omega_{pl}^2(r) = 4\pi n(r)$. Equation 5 has been discretized using the same grid as in the TDLDA calculations. The resulting algebraic equation was solved using conventional methods. The results are shown in Figure 3b. It can be seen that the plasmon resonances obtained using eq 5 are much broader than the TDLDA results in Figure 3a. This is caused by the SCA sampling of a charge density that varies between the bulk value in the center of the shell and zero outside its surfaces. The SCA calculations display a relatively strong absorption peak around 5 eV, which is not seen in the quantum mechanical calculations. This feature is an artificial surface plasmon located in the region of reduced charge density in the surface region of the shell. The Figure shows that the inclusion of a realistic electron-density distribution rather than a simple step-charge density model accounts for the weak red shift of the ω_+ mode observed in the TDLDA calculations. The TDLDA calculations in Figure 3a shows a small size dependence of the ω_- resonant mode. For the smallest nanoshell, this resonant mode is slightly blue shifted with respect to the energy predicted by eq 1. As the size of the nanoshell is increased, the ω_- resonant mode red shifts continuously until it reaches the value given by eq 1. This effect is absent in the SCA results, which indicates that the SCA may break down for very small nanoshells where quantum size effects are expected to be strong. A more detailed investigation of how the energies of the plasmon resonances of nanoshells with

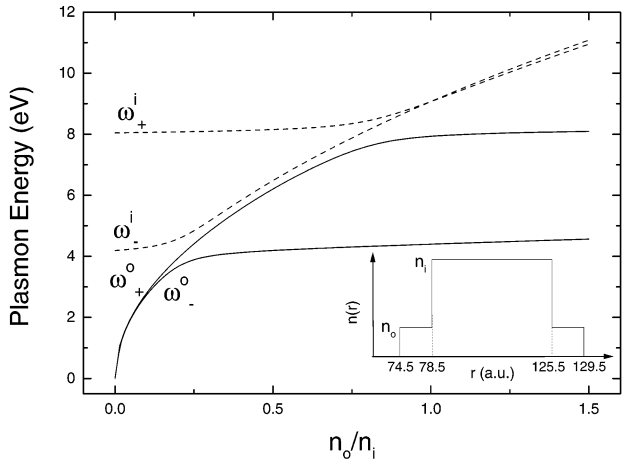

Figure 4. Calculated plasmon energies $\omega_{\pm}^{i}$ and $\omega_{\pm}^{o}$ for nanoshells with a simple stepped surface-charge electron density. The plasmon energies are calculated as a function of n_o/n_i, where n_o is the surface-charge density and n_i is the interior electron density. The charge-density model is schematically indicated in the inset.

the same aspect ratio depend on overall nanoshell size will be presented elsewhere. Before attempting an experimental detection of such a small size dependence, it will be crucial to include in our formalism other physical mechanisms that can cause a size dependence such as the effects of retardation, d electrons, dielectric screening, and possibly other electronic effects.

The data in Figure 1 shows that for the largest nanoshells several peaks at energies around the bulk plasmon frequency are observed. These features can be qualitatively understood from a simple step model of the surface-charge-density profile of the nanoshells. When the density of electrons is approximated by step functions, the integral equation (eq 5) reduces to a set of linear equations.[21] When the surface charge is modeled as in the inset of Figure 4, eq 5 reduces to a set of four linear equations, and consequently, four plasmon modes are expected. The curves in Figure 4 show the energies of these plasmon resonances as a function of the ratio between the surface-charge density and interior-charge density n_o/n_i. For small n_o, there is very little coupling between the plasmon modes associated with the inner charge density n_i and the surface-charge density n_o. The energies of the two dipolar plasmon resonances associated with each charge-density distribution are essentially given by the SCA result (eq 1) with ω_s evaluated for the two charge densities n_o and n_i and a geometry of (78.5, 125.5) au. As n_o increases, the plasmon modes interact, resulting in more complicated, hybridized plasmon modes. For $n_o = n_i$, the physical situation is a homogeneous nanoshell of a (74.5, 129.5) geometry. For this n_o, only three different plasmon energies are present. The two with the lowest energy are the two dipolar plasmon resonances for a nanoshell of geometry (74.5, 129.5). The high-energy modes collapse into a degenerate mode located exactly at the bulk plasmon energy, and their spectral weights go to zero. If we further increase n_o, then the degeneracy of the two high-energy modes is lifted, and their spectral weights become finite. From Figure 4, it can be seen that a ratio of about 1.1 between n_o and n_i most suitably fits the TDLDA calculations for the (76.5,127.5) au nanoshell. For this ratio, the step model predicts energies of 4.25 and 8 eV for the lower-energy modes and an energy of about 9.5 eV for the higher-energy modes, in qualitative agreement with the results of Figure 3a. Such an $n_o \neq n_i$ ratio is in reasonable agreement with the charge-density profile shown in the inset of Figure 3, which includes strong Friedel oscillations near the surfaces.

In conclusion, we have shown that the optical properties of real-size metallic nanoshells can be modeled using a jellium model and TDLDA. We have implemented the TDLDA for a series of nanoshells with an overall diameter ranging from 4 to 36 nm. For all nanoshells considered in this study, we found that the optical response is dominated by two collective resonant plasmon modes. The energy of the plasmon modes varies with the ratio of shell thickness to particle radius in a manner similar to what was predicted earlier using classical Mie scattering and a semiclassical model applied to a nanoshell with uniform electron density. The strong Friedel oscillations near the surfaces of the shell were found to induce additional collective modes at energies comparable with the bulk plasmon energy.

Acknowledgment. We thank Professor N. J. Halas for valuable discussions and comments. This work was supported by the Robert A. Welch foundation under grant C-1222 and by the Multi-University Research Initiative of the Army Research Office.

References

(1) Alivisatos, A. P. *Science (Washington, D.C.)* **1996**, *271*, 1690.
(2) Kreibig, U.; Vollmer, M. *Optical Properties of Metal Clusters;* Springer-Verlag: Berlin, 1995.
(3) Averitt, R. D.; Sarkar, D.; Halas, N. J. *Phys. Rev. Lett.* **1997**, *78*, 4217−4220.
(4) Oldenburg, S.; Averitt, R. D.; Westcott, S.; Halas, N. J. *Chem. Phys. Lett.* **1998**, *288*, 243−247.
(5) Jackson, J. B.; Halas, N. J. *J. Phys. Chem. B* **2001**, *105*, 2743−2746.
(6) Graf, C.; van Blaaderen, A. *Langmuir* **2002**, *18*, 524−534.
(7) Sun, Y.; Mayers, B. T.; Xia, Y. *Nano Lett.* **2002**, *2*, 481−485.
(8) Aden, A. L.; Kerker, M. *J. Appl. Phys.* **1951**, *22*, 1242−1246.
(9) Neeves, A. E.; Birnboim, M. H. *J. Opt. Soc. Am. B* **1989**, *6*, 787−796.
(10) Sarkar, D.; Halas, N. J. *Phys. Rev. E: Stat. Phys., Plasmas, Fluids, Relat. Interdiscip. Top.* **1997**, *56*, 1102−1112.
(11) Oldenburg, S. J.; Jackson, J. B.; Westcott, S. L.; Halas, N. J. *Appl. Phys. Lett.* **1999**, *75*, 2897−2899.
(12) Enderlein, J. *Appl. Phys. Lett.* **2002**, *80*, 315−317.
(13) Hale, G. D.; Jackson, J. B.; Shmakova, O. E.; Lee, T. R.; Halas, N. J. *Appl. Phys. Lett.* **2001**, *78*, 1502−1504.
(14) Sershen, S.; Westcott, S. L.; West, J. L.; Halas, N. J. *Appl. Phys. B* **2001**, *73*, 379−381.
(15) Sershen, S.; Westcott, S. L.; Halas, N. J.; West, J. L. *J. Biomed. Mater. Res.* **2000**, *51*, 293−298.
(16) Sun, Y.; Xia, Y. *Anal. Chem.* **2002**, *74*, 5297−5305.
(17) Jackson, J. B.; Westcott, S. L.; Hirsch, L. R.; West, J. L.; Halas, N. J. *Appl. Phys. Lett.* **2003**, *82*, 257−259.
(18) Mukhopadhyay, G.; Lundqvist, S. *Il Nuovo Cim. B* **1975**, *27*, 1−17.
(19) Mukhopadhyay, G.; Lundqvist, S. *J. Phys. B: At. Mol. Opt. Phys.* **1979**, *12*, 1297−1304.
(20) Ostling, D.; Apell, P.; Rosen, A. *Europhys. Lett.* **1993**, *21*, 539−544.
(21) Ostling, D.; Apell, S. P.; Mukhopadhyay, G.; Rosen, A. *J. Phys. B: At. Mol. Opt. Phys.* **1996**, *29*, 5115−5125.
(22) Vasvari, B. *Z. Phys. B: Condens. Matter* **1996**, *100*, 223−229.
(23) Prodan, E.; Nordlander, P. *Chem. Phys. Lett.* **2001**, *349*, 153−160.
(24) Prodan, E.; Nordlander, P. *Chem. Phys. Lett.* **2002**, *352*, 140−146.
(25) Prodan, E.; Lee, A.; Nordlander, P. *Chem. Phys. Lett.* **2002**, *360*, 325−332.
(26) Prodan, E.; Nordlander, P.; Halas, N. J. *Chem. Phys. Lett.* **2003**, *368*, 94−101.
(27) Nordlander, P.; Prodan, E. *Proc. SPIE* **2002**, *4810*, 91−98.

(28) Perdew, J. P.; Wang, Y. *Phys. Rev. B* **1992**, *45*, 13244−13249.
(29) The equations for the local polarizability, eqs 3 and 4, are the same as the ones used in ref 24. In the present paper, the equations are written in terms of Π rather than $\tilde{\Pi}$.
(30) Zangwill, A.; Soven, P. *Phys. Rev. A: At., Mol., Opt. Phys.* **1980**, *21*, 1561−1572.

NL034030M